e-Research Reports
of Museum Burg Golling
Vol. 3 | 2022

MUSEUM BURG GOLLING
Das regionale WeltenMuseum

The Binghöhle, an epigene cave of Pleistocene origin and its history revealed by U/Th dating (Streitberg, Franconian Alb, Bavaria, Germany)

Stephan Kempe[1], **Sebastian V. Wiesler**[1] & **Katja Huhn**[2]

[1] TU-Darmstadt, Institut für Angewandte Geowissenschaften, Schnittspahnstraße 9, 64287 Darmstadt, Germany

[2] Touristinformation Wiesenttal, Binghöhle Streitberg, Forchheimer Straße 8, 91346 Wiesenttal, Germany

kempe@geo.tu-darmstadt.de

OPEN ACCESS

Published: 06.09.2022

Citation: Kempe, S., Wiesler, S. V. & Huhn, K. (2022): The Binghöhle, an epigene cave of Pleistocene origin and its history revealed by U/Th dating (Streitberg, Franconian Alb, Bavaria, Germany). — e-Research Reports of Museum Burg Golling 3: 1-11.

Published by
Museum Burg Golling
Markt 1
5440 Golling a.d. Salzach
AUSTRIA
office@museumgolling.at
www.museumgolling.at

Binghöhle | U/Th dating | epigene cave genesis | sedimentology | 3D-scanning
Binghöhle | U/Th Datierung | epigene Höhlengenese | Sedimentologie | 3D-Scannen

Abstract: The Binghöhle — named after Ignaz Bing, who discovered the cave in 1905 and opened it as a show cave in 1906 — is situated at Streitberg, Community of Wiesenttal, in the northern Franconian Alb, State of Bavaria, Germany. The cave has formed in Upper Jurassic (Malm β) carbonates of the banked lagoonal facies. It consists of one meandering passage with only few enlargements. Scallops attest to its epigenic origin by turbulently flowing water. In 2014 the cave was 3D-scanned with a FARO S120 and four speleothem samples were U/Th-dated. Sediments were sampled for grain-size analyses, scallops were measured and evaluated statistically for flow rates and data were analyzed. Speleothems yielded ages of 80, 104, 190 and 225 ka BP, corresponding with MIS 5a, 5c and (most likely) 7a and 7c, respectively. Their relevance as to the development of the cave is discussed and the geological history of the cave is reconstructed.

Kurzfassung: Die Binghöhle — benannt nach Ignaz Bing, der die Höhle 1905 entdeckte und sie 1906 als Schauhöhle öffnete — liegt bei Streitberg (Kreis Wiesenthal in der nördlichen Fränkischen Alb, Bayern, Deutschland). Die Höhle bildet sich in den lagunären, gebankten Kalken des Malm β (Oberer Jura). Sie besteht aus einem mäandrierenden Gang mit wenigen Erweiterungen. Gut erhaltene Fließfacetten bezeugen ihre epigene Genese durch turbulent fließendes Wasser. 2014 wurde die Höhle mit einem FAROS S 120 3D-gescannt und vier Speläothem-Proben mit der U/Th Methode datiert. Sedimentproben wurden auf ihre Korngrößenverteilung untersucht und die Größe der Fließfacetten zur Bestimmung der Fließgeschwindigkeit genutzt und die Daten zusammengefasst. Die Speläotheme ergaben Alter von 80, 104, 190 und 225 ka BP, die jeweils den MIS 5a, 5c und (vermutlich) 7a und 7c entsprechen. Ihre Bedeutung für die Entwicklung der Höhle wird erläutert und die geologische Geschichte der Höhle rekonstruiert.

Introduction

Germany has a large variety of caves of different geological stratigraphy, different host rock composition, different origin, different age, different paleontological importance, different speleothem content and different preservation status (e.g., Kempe & Rosendahl, 2008). The northern Franconian Alb was one of the areas that attracted attention of romantic artists, bone-hunters for medical purposes and landscape gardeners early on in history. Here, many caves occur in a relatively small area (compare Kempe et al., 2022, Fig. 1) stratigraphically developed in the Upper Jurassic (Malm) carbonates. Most of these are hypogene in origin and possibly very old, i.e., dating from the Upper Cretaceous (e.g., Kempe et al., 2017). Among these caves is the Binghöhle (Brand et al., 2006) an exotic because of its epigene origin by turbulently flowing water (**Fig. 1**).

Binghöhle

The cave was discovered by Ignaz Bing, a factory owner from Nürnberg, in 1905. He had it excavated and opened it as a show cave in 1906, electrifying it the next year. In 1937 the upper 70 m of the cave were excavated, allowing for an exit of the cave (Illmann, 2006). The cave is situated within the Malm β (Schabdach, 2006), which is characterized by meter-thick banks of limestone, separated by thin layers of marl (**Fig. 2**). The fine-grained limestone originated in the shallow lagoons between sponge- and stromatolite-reefs in the warm upper Jurassic epicontinental sea. These reefs, often later dolomitized, form prominent hills nearby and are also cave-bearing (e.g., the nearby Geisloch, Kempe et al., 2022). Fossils of brachiopods and echinoderms and other marine organisms are common in certain strata and protrude from the cave walls because of their silicification and hence insolubility.

The cave today crosses an eastern flank of the Malm plateau near Streitberg with an entrance at 375 m above sea level. Both of its ends are located about 50 m above the valley (Schauertal) to its east and consists of a single, ca. 300 m long (Preu, 2006: 51), meandering passage, often rectangular in cross-section with scalloped walls (**Fig. 2**). The scallops attest to a N-S directed paleo-flow, even though the cave demonstrates a low angle of slope, amounting to only 0.5 % (Preu, 2006). Both entrances were originally closed by sediment and flowstone that also nearly blocked the cave at places. Bones of Pleistocene fauna are missing, which is strange, given the many bone-caves in the area. The passages strike NW-SE (»hercynian«) and SW-NE (»variscan«) directions (**Fig. 3**) that are also found in the local photo-lineations of the northern Franconian Alb (compare Fig. 1 in Kempe et al., 2022). To obtain additional information on the speleogenesis and its history, the cave was scanned, scallop sizes were surveyed, speleothems were sampled for U/Th dating and sediments collected for grain analysis. Part of these data were summarized in his bachelor thesis by Sebastian Wiesler (2016).

Methods

A FARO Laser Scanner Focus3D S 120 was used (**Fig. 4**) to scan the cave (FARO Technologies Inc., 2011; Kempe & Bauer, 2017). It uses a 20 mW infrared laser of 905 nm and measures distances by phase shift between two reflected pulses of different wavelength. A reflection value is stored in addition to spherical coordinates that are automatically transformed to cartesian coordinates. Built-in level, altimeter and compass help to station the instrument. The scanner rotates 360° vertically and 180° horizontally and was set to collect about 44 million points per station. 15 cm-reference balls (**Fig. 4**) are used to link one station to the next by the FARO program SCENE (for details of the measurement method compare Kempe et al., 2022). The concatenated point cloud of the Binghöhle is shown in Fig. 5 at an angle. In addition, the visible joints in the cave were mapped (**Fig. 1**). Scallop sizes were measured at ten sites in in the cave

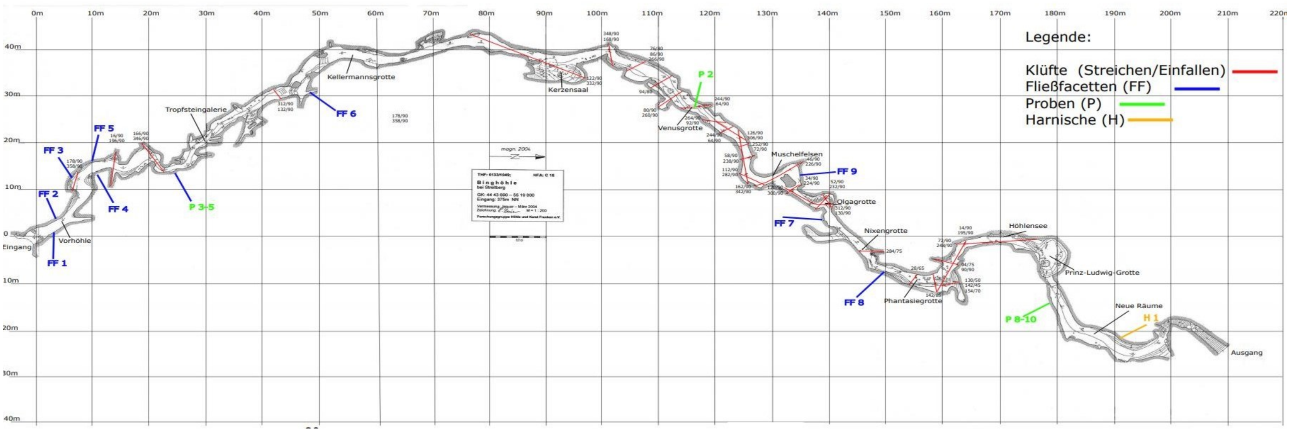

Fig. 1: Map of Binghöhle. Downhill is to the left (south). Map by Forschungsgruppe Höhle und Karst Franken e. V. (Brand et al., 2006; altered by Wiesler, 2016). Red: joints and faults; blue: measurement sites of scallops (Fließfacetten); green: sediment sampling sites. | **Abb. 1**: Karte der Binghöhle: Bergab ist nach links (Süden). Karte der Forschungsgruppe Höhle und Karst Franken e. V. (Brand et al., 2006; verändert von Wiesler, 2016). Rot: Klüfte und Störungen; blau: Messstellen der Fließfacetten; grün: Sedimentproben.

Fig. 2: Typical passage cross-section of the Binghöhle. Note scallops on left side and banked strata. Photo: S. Kempe. | **Abb. 2**: Typischer Querschnitt des Ganges der Binghöhle. Deutlich sind die Fließfacetten (links) und die gebankte Lagerung zu erkennen. (Foto: S. Kempe).

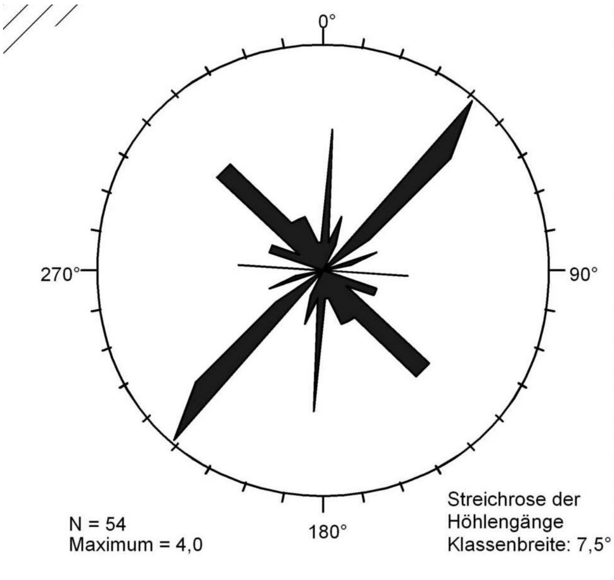

Fig. 3: Diagram of direction of passages of Binghöhle (Wiesler, 2016, after Kaulich & Schaaf, 1980). | **Abb. 3**: Diagramm der Gangrichtungen der Binghöhle (Wiesler, 2016, after Kaulich & Schaaf, 1980).

Fig. 4: The FARO 120 in action in the Binghöhle. Note the three reference balls at the floor and the scallops on the ceiling and walls. Photo: S. Kempe. | **Abb. 4**: Der FARO 120 beim Scannen in der Binghöhle. Beachte drei Referenz-Bälle auf dem Boden und die Fließfactten an den Wänden. Foto: S. Kempe.

Scallop site No	N of measurements	Mean (cm)
1	39	5.5
2	60	5.4
3	33	3.7
4	60	4.9
5	24	3.8
6	33	4.2
7	128	5.1
8	66	4.9
9	93	3.7
Total	536	4.58 ± 0.73

Tab. 1: Sizes of scallops at nine different sites in the Binghöhle (Wiesler, 2016). For location of sites see Fig. 1. | **Tab. 1**: Größe der Fließfacetten an neun verschiedenen Stellen der Binghöhle (Wiesler, 2016). Für Lage der Messstellen siehe Abb. 1.

(locations marked in **Fig. 1**) and averaged to determine paleo flow velocity and discharge (**Tab. 1**).

Sediments were sampled at three locations (see **Fig. 1**). Seven samples were analyzed for their grain-size according to DIN 18123, 2011 (**Tab. 2**). Each sample was about 100 g. The coarser sediments were sieved, while the finer sediments were also submitted to aerometry. Furthermore, calcium-carbonate concentrations were measured by the Scheibler-Method on four samples with four or five repeats each (DIN 18129, 2011).

Four speleothems (Bing 2 to 5) were collected at prominent sites for U/Th dating. These were dated by Jens Fohlmeister at Heidelberg, Institut für Umweltphysik, using an Inductively Coupled Plasma Source Quadrupole Mass Spectrometer (ICPQMS, ThermoFisher iCAP-Qs) (Arps, 2017), financed by a grant from the Wiesenttal Community, the owner of the show cave (**Tab. 3**).

Results

The 3D scan allowed a closer look at the tectonic structure of the cave: The passages of the Binghöhle mostly follow bedding planes. The map (**Fig. 1**) shows that joints were not the guiding tectonic elements in many of the passage sections (**Fig. 6**). In these sections, the initial cavity seemingly formed solely along

Fig. 5: Slanted view of point cloud of Binghöhle seen from the ESE. Green arrow (Y, lower right) is pointing N. Note that the passage shows irregular appendices, possibly remains of its early phreatic hypogene phase. | **Abb. 5**: Schrägansicht auf die Punktwolke des Binghölhen-3D Models aus ESE. Grüner Pfeil (Y-Richtung unten rechts) zeigt nach N. Erkennbar sind die unregelmäßigen Erweiterungen, die möglicherweise auf frühe phreatische, hypogene Phasen der Höhlenentwicklung zurückgehen.

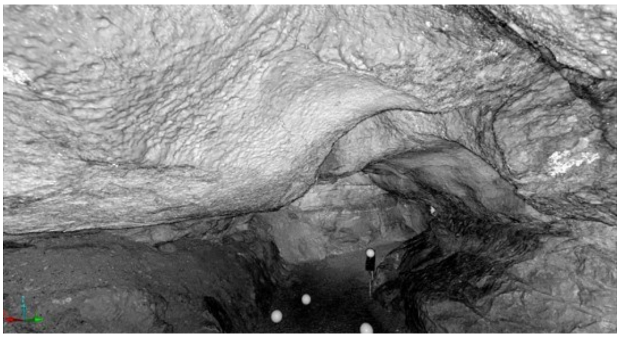

Fig. 6: This point-cloud picture depicts a section of the cave passage that developed along a prominent bedding plane without a ceiling joint. Dissolution (note scallops) enlarged the cave both upward into the overlying limestone bench as well as downward into the bench (or benches) below. | **Abb. 6**: Dies Punktwolkenbild zeigt einen Abschnitt des Höhlenganges, der sich entlang einer wichtigen Schichtfuge ohne den Beitrag einer Deckenkluft entwickelt hat. Die Korrosion (siehe die Fließfacetten) hat den Gang sowohl in die hangende als auch die liegende Kalkbank vergrößert.

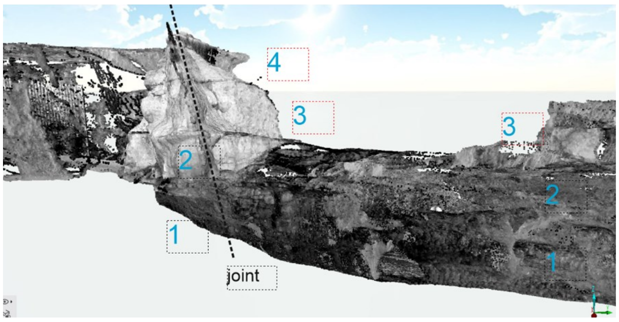

Fig. 7: Point cloud picture of a section of Binghöhle illustrating tectonic details (N is to the right). Flow was from right to left. Numbers refer to individual benches, separated by bedding planes. The cave was initiated along the bedding plane 3/2 and then jumped upward along a N-dipping joint to follow the bedding plane on top of bench 4. | **Abb. 7**: Blick von außen und aus Osten auf die Punktwolke des 3D-Models eines Abschnittes der Binghöhle zur Darstellung tektonischer Details (Nord ist rechts). Der Durchfluss war von rechts nach links. Die Nummern beziehen sich auf einzelne Bänke, die durch Schichtflächen getrennt sind. Die Höhle entwickelte sich an der Schichtfuge 3/2 und sprang dann - entlang eine N-fallenden Kluft - auf die Schichtfläche oberhalb der Bank 4.

bedding planes. Since the bedding is dipping steeper than the cave, joints were often used to guide the initial phreatic tube to a higher bedding plane (**Fig. 7**). The initial phreatic tubes (anastomoses) are preserved in the ceiling at several places in the cave (**Fig. 8**).

The walls of the Binghöhle are scalloped throughout (**Fig. 6**, **9**). Scallops form due to the turbulence in the flowing water and their size is a function of velocity while their asymmetric shape is a function of direction (the flatter side points down-current) (Curl, 1974; **Fig. 10**).

Preu (2006) had previously measured scallop-sizes and deduced flow velocities and flow rates (1550 l/s). In his bachelor thesis Wiesler (2016) measured scallops at many more places (**Fig. 1**) and calculated means (**Tab. 1**; **Fig. 10**). In the Nixengrotte (site 7, Fig. 1), scallops averaged 5.2 cm in size yielding a velocity of 28 cm/s and a flow rate in a 2 m wide tube of 880 l/s. This is calculated for present water temperature; for temperatures near freezing the flow velocity would be somewhat smaller. Scallop sizes should be measured at the site with the smallest cross-section. This is, however, difficult to do, because the floor of the cave contains a fill of an unknown thickness and cross-sections are irregular in shape and size. This explains the difference between the estimates of Preu (2006) and Wiesler (2016). Thus, a discharge of about 1 m^3/s may be a sufficiently exact assumption.

Shortly above the present entrance, the cave passage shows a prominent meander. On its slip-off slope scallops measure 4.9 cm on average and on the eroding bank 3.8 cm on average, illustrating the velocity difference between the two banks of a meander. **Tab. 2** lists the results of the grain size analyses. Sample 2 (**Fig. 11**) and the samples 3 to 5, comprising a small profile (**Fig. 12**), are coarser grained than samples 8 to 10 (**Fig. 13**), also forming a profile. The coarser samples from the first profile show a »fining upward« tendency (**Fig. 12**). Similarly, the calcium carbonate content increases from about 0.77 to 13.6 %.

Sample #	Weight (g) dry/wet	above floor, cm	$CaCO_3$ %	Description
2	86.4	112	2.76 ± 0.72	Coarse sand, fine gravel, silty, fine-sandy, middle-sandy
3	100.2	60	13.6 ± 2.73	Fine gravel, coarse sand, silty, fine-sandy, middle sandy
4	82.9	50	8.13 ± 0.25	Fine gravel, coarse sand, middle sandy
5	98.1	15	0.77 ± 0.16	Sand, silt, fine gravely
8	76.9/42.2	137	n.d.	Silt, clay, fine sandy
9	91.6/47.4	107	n.d.	Clay, silt, fine sandy
10	114/45	80	n.d.	Silt, clay, fine sand

Tab. 2: Grain size analyses. For sample location see Figure 1. Samples 3-5 and 8-10 are profiles. $CaCO_3$ content was determined by the Scheibler-Method (Wiesler, 2016). | **Tab. 2**: Korngrößenanalysen der Sedimente der Binghöhle. Für Probenstellen siehe Abb. 1. Proben 3-5 und 8-10 sind Profile. Kalkgehalt wurde mit der Scheibler-Methode bestimmt. Daten nach Wiesler, 2016.

LabNr.	Sample	^{238}U (ng/g)	Error (abso.)	^{232}Th (ng/g)	Error (abso.)	$^{230}Th/^{238}U$ (act.ratio)	Error (abso.)	$^{230}Th/^{233}U$ (act.ratio)	Error (abso.)
6843	Bing 2	80,21	0,23	1,1278	0,0073	1,238	0,014	269,6	3,4
6844	Bing 3	88,99	0,26	3,0353	0,0271	1,914	0,034	171,2	3,3
6845	Bing 4	195,32	0,48	3,451	0,028	2,207	0,033	382,8	6,3
6846	Bing 5	71,38	0,25	9,235	0,055	1,330	0,016	31,32	0,37

Sample	$\delta^{234}U$ corr. (‰)	Error 2σ abso. (‰)	Age uncorr. (ka)	Error (ka)	Age corr. (ka)	Error (ka)	$\delta^{234}U$ initial (‰)	Error 2σ abso. (‰)
Bing 2	332,5	5,7	225,48	8,41	225,2	8,62	628,4	18,1
Bing 3	1077,0	11,7	190,2	7,9	189,9	8,26	1842,0	46,2
Bing 4	2286,1	13,0	104,0	2,4	103,9	2,4	3065,9	27,0
Bing 5	1411,1	27,2	81,4	1,3	80,0	1,8	1769,0	35,3

Tab. 3: Results of the U/Th dating of samples from speleothems from the Binghöhle. Measurements by J. Fohlmeister, Heidelberg. | **Tab. 3**: Ergebnisse der U/Th Datierung der Speläotheme aus der Binghöhle. Messungen durch J. Fohlmeister, Heidelberg.

Their coarse nature is indicative of fluvial sediments, deposited in the cave when it served as a water course. The coarser particles contain silicified fossil fragments and bean-ore nuggets (**Fig. 14**). These fragments have already been described by Brand (2006), who, in addition, isolated teeth and bones from small rodents (Family *Arvicolidae*, genera *Arvicola*, *Microtus* and *Clethrionomys*) and insectivores (*Sorex* and *Talpa*) with a few other remains (*Glis*, ?*Mustela*, reptile and even fish remains, plus gastropod fragments). Most of these remains were found in the sediments of the entrance section and are of younger age. Mammal remains from the fluvial sediments are less common (?*Minomys*, *Apodemus*, ?*Arvicola cantiana*, *Microtus*) and are tentatively Middle Pleistocene in age (Brand, 2006: 30).

The fine-grained sediments of the second profile derive from a set of speleothem layers (**Fig. 15**). The upper two samples in between the three speleothem layers have a similar grain size curve with roughly equal clay and silt contents. They are red brown in color. These sediments are clearly not fluvial but seem to have been brought in with seepage water in between pauses of speleothem formation. Sample 10, from below the lower speleothem layer, is lighter in color and has more silt, less clay and a noticeable fine sand fraction. It could be the top of the sediment that once filled the passage before being dug out to extent the show cave. Its grain size is characteristic of loess. Unfortunately, Wiesler (2016) did not analyze these layers for their carbonate content.

The texture of the sediment that once filled the passage below the speleothem layers is that of a mudflow or solifluction soil with large rock fragments. However, this layer has not been investigated sedimentologically yet.

The results of the U/Th dating are given in **Tab. 3**. All samples had a high enough uranium and a low enough detrital thorium content to allow calculation of meaningful ages. The dates for the speleothem profile in **Fig. 15** were (from bottom to top): Bing 3: 189.9 ± 7.9 ka BP, Bing 4: 103.9 ± 2.4 ka BP and Bing 5: 80.0 ± 1.3 ka BP, thus representing a sequence of layers in stratigraphic order, covering 100,000 years. These layers are interspersed by seepage derived sediments. As only one sample was dated per layer, the exact time span that each of the layers represents, remains unknown. When looking at them on **Fig. 15**, each of them is separated into several benches that could be dated individually. Sample Bing 2 yielded the oldest date: 225.2 ± 8.41 ka BP. This is the most interesting sample yet dated in view of the history of the Binghöhle. **Fig. 16** illustrates why: The wall speleothem itself is scalloped. It therefore predates the last cave -forming event when turbulent flow enlarged the cave, corroding older speleothems.

Discussion

The Binghöhle for most of its length is a meandering, subterraneous water course of similar cross-section (**Fig. 1**). It follows

Fig. 8: Anastomosis along a bedding plane (faintly visible above rock hammer on the left). Photo: S. Wiesler. | **Abb. 8**: Blick in die Anastomose entlang einer Schichtfuge (gerade sichtbar oberhalb des Geologenhammers auf der linken Seite).

Fig. 9: Scallops on the east-wall of the Nixengrotte that formed due to turbulence in the flow. The paleo-flow was to the right (S). Rock hammer for scale. Photo: S. Wiesler. | **Abb. 9**: Fließfacetten an der Ostseite der Nixengrotte, die den turbulenten Durchfluss anzeigen (Geologenhammer als Maßstab). Foto: S. Wiesler.

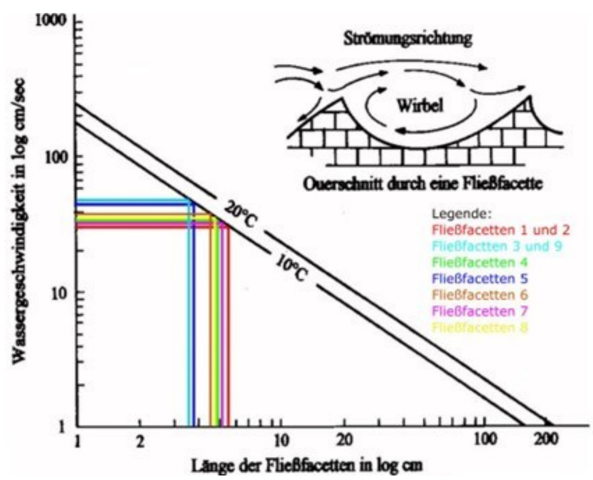

Fig. 10: Log-log plot of the scallop width (x-axis) versus flow velocity (y-axis) (Wiesler, 2016, altered after Curl, 1975). | **Abb. 10**: Doppellogarithmische Darstellung der Abhängigkeit der Fließfacetten-Länge (x-Achse) von der Fließgeschwindigkeit (y-Achse) (Wiesler, 2016, geändert nach Curl, 1975).

bedding planes either along joints or without those. The initial anastomoses are preserved at places. Apparently, the softer marl layers, the substance of the bedding between the banks of the Malm β limestones, were instrumental in allowing the »break-through« of phreatic anastomoses (Dreybrodt, 2008). Overall, the cave has an astonishingly low slope, lower than the dip of the bedding, therefore crossing joints were used to skip bedding planes upward. The presence of scallops on walls and ceiling (the rock floor is nowhere visible) suggest that the cave, when active, was phreatic and not a canyon with a vadose stream at its bottom. Even at the present entrance, there are no signs of a vadose cut-down towards the valley. However, some of the halls, like the »Kerzensaal« and uprising openings along joints do not fit this model. These smaller elements of the cavity may well predate the formation of the water conduit and could be of hypogene origin.

Preu (2006) already calculated, on basis of scallop sizes, that the discharge of the cave must have been in the order of 1 m^3/s or higher. He points out that this is a much larger discharge than the yield of springs of the adjacent Schauertal, the present drainage of the plateau behind the Binghöhle. An approach to estimate the current potential discharge area needed, is using average discharge rates of the Danube tributary area. Currently (but using the pre-climate-change data, i.e., for the period 1966-71), the Danube has a discharge of 458 mm/a at Hofkirchen, a station above and excluding Vils, Ilz and Inn (Kempe et al., 1981). To generate a discharge of 1 m^3/s, it would need a tributary area of 70 km^2 (**Fig. 17**), while the immediate area of the basin north of the Binghöhle, the Störnhof basin, amounts to only 3.8 km^2. There are three assumptions we can make, if we accept Curl's experimental results (Curl, 1975):

1. The discharge was about 20 times higher than today (hardly likely).
2. The tributary area used to be much larger than today (which implies fast landscape changes).
3. The discharge operated only for a few weeks per year (like after the spring snow melt?).

Assumption 2 implies that several of the smaller valleys that now transect the area north of the Binghöhle (**Fig. 16**) have formed within the last 200,000 years, otherwise such a large tributary area is not realistic. But the Binghöhle itself is witness to such short-term valley enlargement because its upper continuation was cut-off 200,000 year ago by the adjacent Schauertal (see below). It is not the aim of this paper to analyze the processes that have led to this development, but certainly limestone dissolution is not fast enough to cause the fast back-cutting of the small valleys. We have to invoke other processes, such as sliding of the Malm β on the underlying Dogger clay, the Ornatenton (Oxfordian). Local dip and permafrost could have led to the fast sliding of Malm blocks towards the Wiesent valley, where these were then removed by erosion. These conclusions are highly hypothetical but illustrate how the dating of speleothems can lead to interesting questions of landscape evolution. We can now sketch the history of the Binghöhle with the data presented so far:

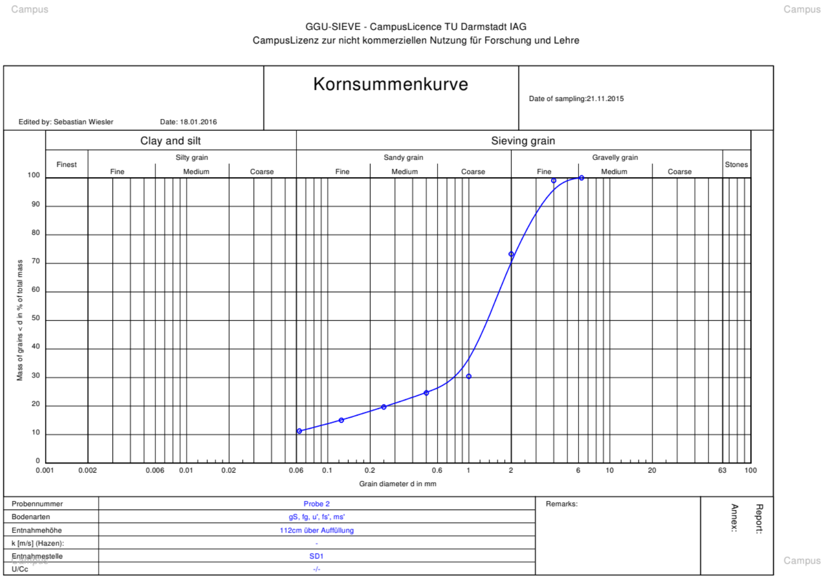

Fig. 11: Grain size composition of sample 2 (Wiesler, 2016). | **Abb. 11**: Korngrößenverteilung der Sedimentprobe 2 (Wiesler, 2016).

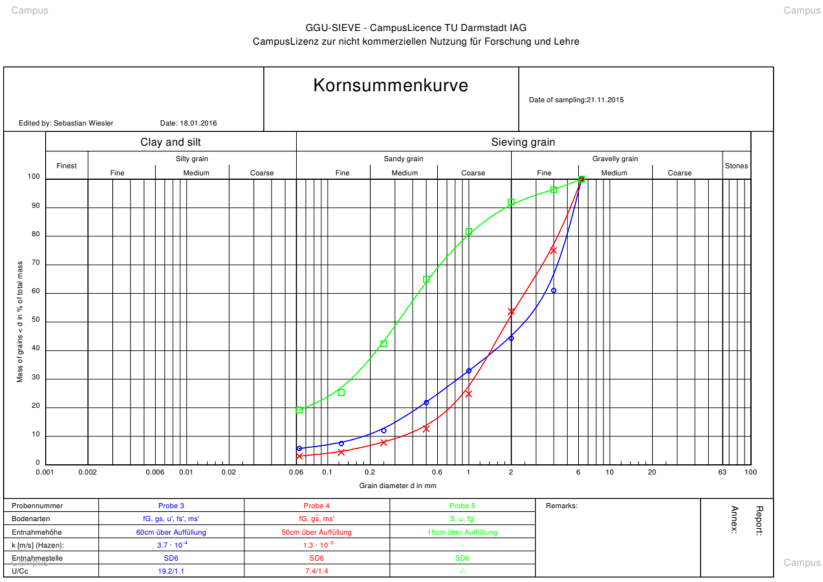

Fig. 12: Grain size composition of profile with (from bottom to top) sample 5 (blue), 4 (red) and 3 (green) (Wiesler, 2016). | **Abb. 12**: Korngrößenverteilung des Sedimentprofils (von unten nach oben). Blau: Probe 5; rot: Probe 4; grün: Probe 3 (Wiesler, 2016).

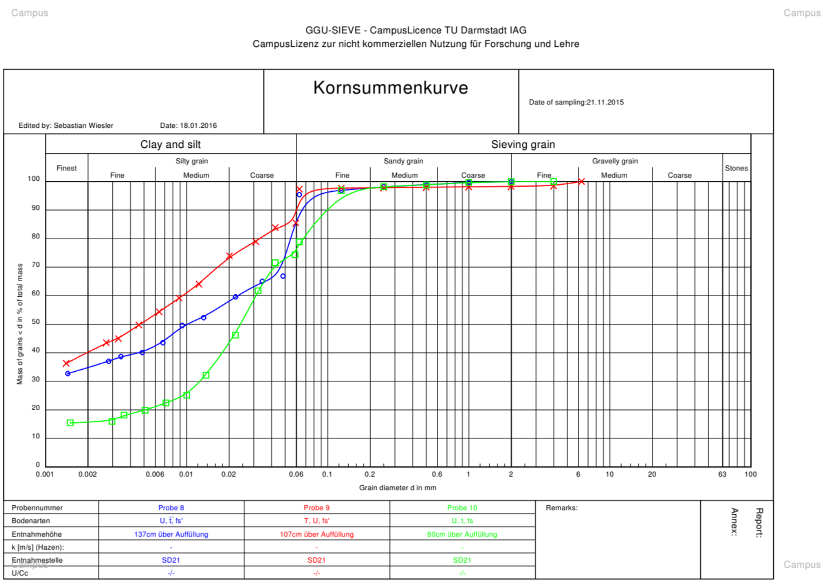

Fig. 13: Grain size composition of profile with (from bottom to top) sample 10 (green), 9 (red) and 8 (blue) (Wiesler, 2016). | **Abb. 13**: Korngrößenverteilung des Sedimentprofils (von unten nach oben). Grün: Probe 10; rot: Probe 9; blau: Probe 8 (Wiesler, 2016).

Fig. 14: Coarse grains of fluvial sediments: silicified echinoderm fragments (top) and bean ore particles (bottom). Photos: S. Wiesler. | **Abb. 14**: Grobe Körner der fluvialen Sedimente: silifizierte Echinodermata-Fragmente (oben) und kleine Bohnerzkörner (unten). Foto: S. Wiesler.

Fig. 15: Situation of speleothem layers Bing 3 to 5, U/Th dated. The two sediment layers in between are sediment samples 8 (top) and 9 (below). Sediment sample 10 was taken below Bing 5 and on top of the massive mudflow that once filled the passage below, dug-out for the show cave. View S, width ca. 1.5 m. Photo: S. Kempe. | **Abb. 15**: Situation der U/Th-datierten Speläotheme Bing 3 bis 5. Die beiden Sedimentlagen zwischen den Bodensinterlagen sind die Sedimentproben 8 (oben) und 9 (unten). Die Sedimentprobe 10 wurden unterhalb von Bing 5 genommen oben auf der mächtigen Fließerde, die einst den Gang füllte, bevor er für die Schauhöhle abgegraben wurde. Der Blick ist nach S, Bildbreite ca. 1,5 m. Foto: S. Kempe.

Fig. 16: Situation of BING 2, sampled for U/Th dating. It is scalloped and therefore predates the final cave-forming event. Note Swiss pocket-knife for scale. Photo: S. Kempe. | **Abb. 16**: Situation der U/Th-datierten Probe Bing 2. Sie zeigt deutliche Fließfacetten, und wurde daher vor dem letzten, höhlenerweiternden Ereignis abgelagert. Schweizer Taschenmesser als Maßstab. Foto: S. Kempe.

— Small, isolated cavities developed hypogenically at times, when the Franconian Alb was far below the groundwater level (compare the paper on Geisloch, Kempe et al., 2022).
— Once the deepening of the Wisent valley cut through the Malm β, karst water was able to create a system of anastomoses, following bedding planes and joints from N to S. Preexisting hypogenic cavities may have helped to establish the first turbulent flow.
— A continuous, meandering passage was established prior to 230,000 years BP. It transported a substantial volume of water, estimated to be more than 1m^3/s, apparently feeding a large karst spring in the Wisent valley.
— The system fell dry at around 225,000 years BP and speleothem formation commenced. Its sparitic texture suggests slow growth which was possibly caused by a closure of the entrances.
— After 225,000 but before 190,000 years BP, the cave was reactivated as a phreatic stream course and enlarged again by turbulent flow, removing part of the already deposited speleothems.
— After this last cave-enlarging event, the water flow diminished, depositing fluvial sediments, fining upward from fine gravel to coarse sand, indicative of a diminishing stream flow.
— Shortly before 190,000 BP, the developing Schauertal cut into the upper end of the cave. Immediately, mudflows intruded the cave, plugging it firmly. The material was most probably mobilized loess.
— In cupolas above the mudflow, speleothems began to form 190,000 years BP, followed by fine-grained clay and silt deposits and two further speleothem layers dated to 104,000 and 80,000 years BP.

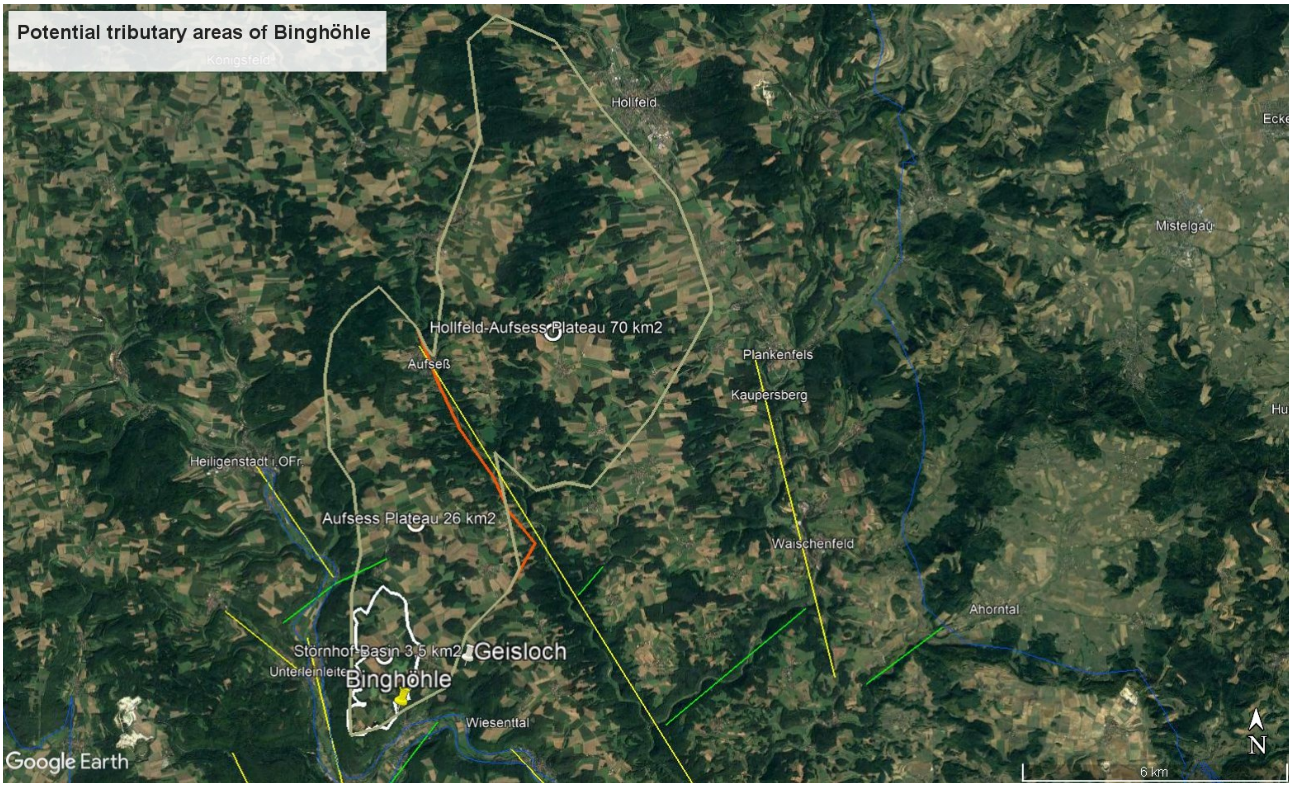

Fig. 17: Google Earth picture of potential discharge areas of the Binghöhle. Green and yellow lines mark prominent photo-lineations. | **Abb. 17**: Google Earth Bild des potentiellen Einzugsgebietes der Binghöhle. Grüne und gelbe Linien markieren Fotolineationen.

Fig. 18: A small stalagmite broken and deposited by cave ice. The stalagmite is too small to have been broken by earthquakes. Photo: S. Kempe. | **Abb. 18**: Kleiner, durch Höhleneis abgebrochener und abgelagerten Stalagmit, der zu klein ist, um durch ein Erdbeben abgeschert worden zu sein. Foto: S. Kempe.

Fig. 19: The Venusgrotte of the Binghöhle and the leaning stalagmites. Probably only the one in the back of the three is original ice damage, the two stalagmites in front have been placed there when clearing the path of the show cave. However, other glacial damage is seen in the foreground. Photo: S. Kempe. | **Abb. 19**: Situationen der Venusgrotte der Binghöhle mit ihren »lehnenden« Kerzenstalagmiten. Vermutlich ist nur der hinterste Stalagmit durch Höhleneis abgeschert worden, die beiden Stalagmiten davor wurden dort platziert als man den Gang für den Betrieb der Schauhöhle freiräumte. Weiterer Glazialschaden ist im Vordergrund zu erkennen. Foto: S. Kempe.

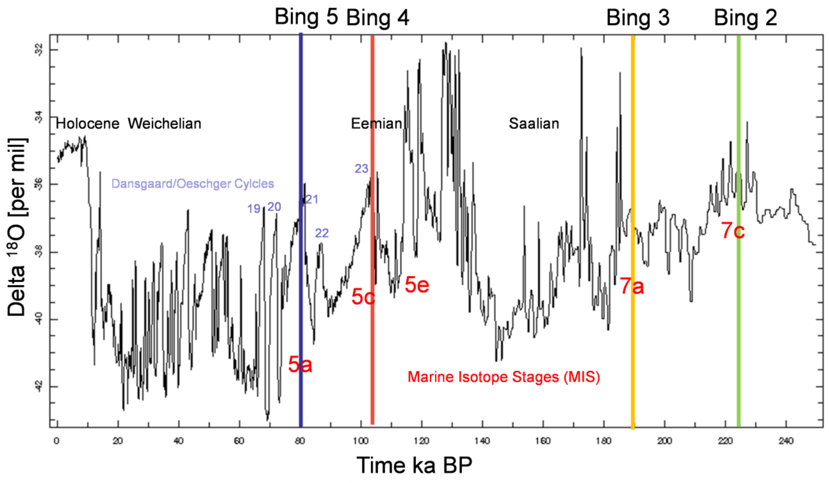

Fig. 20: Comparison of Binghöhle U/Th ages with the GRIP delta 18O ice core data (GRIP, 2021). | **Abb. 20**: Vergleich der U/Th-Daten der Binghöhle mit den GRIP delta 18O Eiskerndaten (GRIP, 2021).

— These speleothem generations began also plugging the stream course at several places, overgrowing the older sediments.

— Bones of Pleistocene mammals were found nowhere in the cave. This could indicate that not only the upper entrance was closed, but that also the lower entrance was inaccessible. One possibility is that a large limestone rock tower slipped towards the Wisent Valley, closing it.

— During the Last Glacial Maximum (LGM, Weichselian or Würmian Glaciation, 24,000 to 18,500 years BP) the cave was filled with ice. Its pressure and slippage destroyed some of the preglacial speleothem generations. Damage in the Binghöhle is not as prominent as in the Geisloch, but nevertheless present (**Fig. 18**). Famous are the »leaning« stalagmites in the Venusgrotte (**Fig. 19**). However, only one of them represents glacial damage, the others appear to be placed there because they had to be moved for the show cave.

— The excavation of the present entrance uncovered only Holocene remains, including bronze-age shards and medieval artefacts (Leja, 2006). Thus, the present cave entrance must have been closed until the end of the LGM. It could have opened by the further slip of the limestone blocks in front of it.

Generally, speleothem growth is correlated with warm and wet periods which sustain active vegetation. **Fig. 20** shows that the dates of Bing 5 and 4 correlate well with the Dansgaard-Oeschger Events 21 and 23, respectively, which are the longest warm Interstadials of the Marine Isotope Stage 5 (MIS), i.e. 5a and 5c. Interestingly, MIS 5e, the last Interglacial (Eemian), is not represented, but it may be hidden in the lower band of this layer (compare **Fig. 15**). For Bing 3 and 2, the comparison with ice core data proves more difficult because the Greenland cores (GRIP or NGRIP) do not resolve well beyond the Eemian. Nevertheless, the two ages can be tentatively correlated with the peaks of the Interstadials MIS 7a and 7c.

Overall, the Binghöhle is geologically an interesting cave meriting further research and dating. The lack of remains of Pleistocene mammals is easily understood. First of all, the cave was an active stream cave and then, between 225 and 190 ka BP, it was plugged by mudflows and the lower entrances were probably buried. Thus, the lack of the presence of bones is evidence for the evolution of the cave itself.

Acknowledgements

3D-scanning was performed by Ingo Bauer and Yasmin Rossmann, Gabi Schubert supervised grain size analyses (all Institute of Applied Geosciences, TU-Darmstadt). The community of Wiesenttal paid for the U/Th dating which was performed by Jens Fohlmeister at the Institute for Environmental Physics, University Heidelberg. Konrad Huhn, the son of Katja Huhn helped Sebastian Wiesler during field work. English was improved by Gregory Middleton.

References

Arps, J. (2017): Towards ε-Precision of U-series Age Determinations of Secondary Carbonate. — Dissertation, Universität Heidelberg. http://archiv.ub.uni-heidelberg.de/volltextserver/23313/1/Dissertation_ Jennifer%20Arps.pdf, looked up 11/2021.

Brand, F. (2006): Was können wir aus den lehmigen Ablagerungen der Binghöhle ablesen? In: Brand, F., Illmann, R., Leja, F., Preu, D. & Schabdach, H.: Die Binghöhle bei Streitberg. Auf den Spuren eines unterirdischen Flusses. — Marktgemeinde Wiesenttal: 28-33.

Brand, F., Illmann, R., Leja, F., Preu, D. & Schabdach, H. (2006): Die Binghöhle bei Streitberg. Auf den Spuren eines unterirdischen Flusses. — Marktgemeinde Wiesenttal.

Curl, R. (1975): Die Ableitung der Fließgeschwindigkeit in Höhlen aus den Fließfacetten. — Mitteilungen des Verbandes der Deutschen Höhlen- und Karstforschung 21/3: 49-55.

DIN 18123 (2011): Baugrund, Untersuchung von Bodenproben — Bestimmung der Korngrößenverteilung.

DIN 18129 (2011): Baugrund, Untersuchung von Bodenproben — Kalkgehaltsbestimmung.

Dreybrodt, W. (2008): Von der Kluft zum Urkanal, Chemie und Physik der Höhlenentstehung. In: Kempe, S. & Rosendahl, W. (Eds.): Höhlen. Verborgene Welten. — Wissenschaftliche Buchgesellschaft Darmstadt: 39-53.

FARO Technologies Inc. (2011): FARO® Laser Scanner Focus3D Manual.

GRIP (2021): http://iridl.ldeo.columbia.edu/SOURCES/.ICE/.CORE/.GRIP/.o18/a-/-a/T/fig-/line/-fig//plotaxislength/432/psdef//plotborder/72/psdef//plotaxislength +432+psdef//plotborder+72+psdef/#options, looked up 12/2021.

Illmann, R. (2006): Die Geschichte der Binghöhle bei Streitberg. In: Brand, F., Illmann, R., Leja, F., Preu, D. & Schabdach, H.: Die Binghöhle bei Streitberg. Auf den Spuren eines unterirdischen Flusses. — Marktgemeinde Wiesenttal: 6-14.

Kaulich, B. & Schaaf, H. (1980): Kleiner Führer zu Höhlen um Muggendorf. — Naturhistorische Gesellschaft Nürnberg e.V., Nürnberg.

Kempe, S., & Bauer, I. (2017): 3-D imaging as a tool to understand speleogenetic processes. In: Moore, K. & White, S. (Eds.): Proceedings 17th Intern. Speleology Congress, Sydney, 22.-30. July, 2017, Vol. 2: 117-121.

Kempe, S. & Rosendahl, W. (2008): Höhlen: verborgene Welten. — Wissenschaftliche Buchgesellschaft Darmstadt, Darmstadt.

Kempe, S., Mycke, B. & Seeger, M. (1981): Flußfrachten und Erosionsdaten in Mitteleuropa. — Wasser und Boden 3: 126-131.

Kempe, S., Bauer, I. & Glaser, S. (2017): Hypogene caves in Germany, geological and geochemical background. In: Klimchouk, A., Palmer, A. N., de Wale, J., Auler, A.S. & Audra, P. (Eds.): Hypogene Karst Regions and Caves of the World, Chapter 21, Springer International Publishing AG, Cham, Switzerland: 329-348.

Kempe, S., Fenzlein, R. & Schabdach, H. (2022): The Geisloch, a well preserved hypogene cave: statistical analysis of pronounced glacial speleothem damage and first U/Th dating of cave bear remains to older than 80 ka BP (Oberfellendorf, Franconian Alb Bavaria, Germany). — e-Research Reports of Museum Burg Golling 4: 1-10.

Leja, F. (2006): Mensch und Höhle, die vorgeschichtlichen und mittelalterlichen Funde aus der Binghöhle bei Streitberg/Ofr. In: Brand, F., Illmann, R., Leja, F., Preu, D. & Schabdach, H.: Die Binghöhle bei Streitberg. Auf den Spuren eines unterirdischen Flusses. — Marktgemeinde Wiesenttal: 38-47.

Preu, D. (2006): Am Anfang war das Wasser, eine kleine hydrologische Exkursion um die Binghöhle. In: Brand, F., Illmann, R., Leja, F., Preu, D. & Schabdach, H.: Die Binghöhle bei Streitberg. Auf den Spuren eines unterirdischen Flusses. — Marktgemeinde Wiesenttal: 51-52.

Schabdach, H. (2006): Einst geschaffen im Jurameer, die Geologie von Streitberg. In: Brand, F., Illmann, R., Leja, F., Preu, D. & Schabdach, H.: Die Binghöhle bei Streitberg. Auf den Spuren eines unterirdischen Flusses. — Marktgemeinde Wiesenttal: 15-17.

Wiesler, S. V. (2016): Speläogenese der Binghöhle, Oberfranken, Bayern. — Bachelor-Thesis, Institute of Applied Geosciences, Technische Universität Darmstadt (unpubl.).